European Journal of Radiology Open 7 (2020) 100240

Contents lists available at ScienceDirect

European Journal of Radiology Open

journal homepage: www.elsevier.com/locate/ejro

Pediatric thoracic mass lesions: Beyond the common

Gunes Orman[a,*], Prakash Masand[a], John Hicks[b], Thierry A.G.M. Huisman[a], R. Paul Guillerman[a]

[a] Edward B. Singleton Department of Radiology, Texas Children's Hospital, 6701 Fannin Street, Houston, TX, 77030 United States
[b] Department of Pathology, Baylor College of Medicine, 1 Baylor Plaza, Houston, TX 77030, United States

ARTICLE INFO

Keywords:
Pediatric
Chest
Thorax
Mass lesion
Neoplasm

ABSTRACT

Thoracic mass lesions can be categorized as originating in one of the three major compartments: a) chest wall and pleura, b) lung parenchyma and airways, c) mediastinum. While some of these, such as lymphoma, are common in both children and adults, others are rare and unique to childhood. The goal of this review is to familiarize radiologists with unusual **but distinctive** mass lesions of the pediatric thorax.

1. Introduction

The spectrum of thoracic mass lesions **encountered in radiology practice differs greatly in children compared to adults.** Metastases from an extra-pulmonary primary malignancy are much more common than primary pulmonary neoplasms in children. Primary pulmonary neoplasms are rare in childhood and less common than non-neoplastic conditions, such as congenital lung malformations [1–3]. Mesenchymal neoplasms are more common than epithelial neoplasms in the pediatric thorax, and certain neoplasms are associated with **genetic disorders** or infections [4].

The most common pediatric thoracic mass lesions include lymphoma, germ cell tumors, neurogenic tumors, foregut cysts, congenital pulmonary airway malformations, vascular malformations, hemangiomas, chest wall sarcomas, pleuropulmonary blastoma, inflammatory myofibroblastic tumor, endobronchial tumors, breast tumors and cardiac tumors. These have been the subject of numerous prior publications [3,5–18] **and are beyond the scope of this review.**

The aim of this review is to **go beyond the common and** familiarize radiologists with **unusual but distinctive** mass lesions involving the pediatric thorax, including **certain** malignant and benign neoplastic lesions and non-neoplastic proliferative and hamartomatous lesions. We will discuss **these** lesions based upon their primary **compartmental** location **(chest wall/pleura, lung parenchyma/airways, mediastinum)** or presumed site of origin if multi-compartmental.

2. Chest wall and pleura

2.1. Mesenchymal hamartoma of the chest wall

Mesenchymal hamartoma of the chest wall, also known as benign mesenchymoma, infantile osteochondroma, osteochondrosarcoma, and infantile cartilaginous hamartoma, is a benign lesion that usually presents as a deforming chest wall mass in an infant or young child [19]. This lesion accounts for 0.03 % of primary bone tumors [20]. It typically arises along the ribs and is characterized by a benign proliferation of precursors of bone tissue with a prominent cartilaginous component, oval to spindled mesenchymal cells with no atypia or abnormal mitotic activity, smooth muscle, and hemorrhagic cavities with osteoclast-like giant cells, imparting aneurysmal bone cyst-like appearance [19,21]. It may be multicentric and/or bilateral. Chest radiography (CXR) shows a partially calcified mass of the chest wall involving one or more ribs. The mass is typically well-delineated and often lobulated with bizarre remodeling or enlargement of the involved rib(s) [21]. Computed tomography (CT) (Fig. 1) and magnetic resonance imaging (MRI) may show mineralized matrix and hemorrhagic cystic components [22]. Differential diagnosis include osteosarcoma or chondrosarcoma [20]. The size of the mass may decrease even without treatment and prognosis is excellent. However, if compressive effects result in cardiac or pulmonary compromise or if the mass is physically deforming, surgical excision of the lesion is recommended [22].

* Corresponding author.
E-mail addresses: gxorman@texaschildrens.org (G. Orman), pmmasand@texaschildrens.org (P. Masand), MJHICKS@texaschildrens.org (J. Hicks), huisman@texaschildrens.org (T.A.G.M. Huisman), rpguille@texaschildrens.org (R.P. Guillerman).

https://doi.org/10.1016/j.ejro.2020.100240
Received 16 December 2019; Received in revised form 8 April 2020; Accepted 5 June 2020

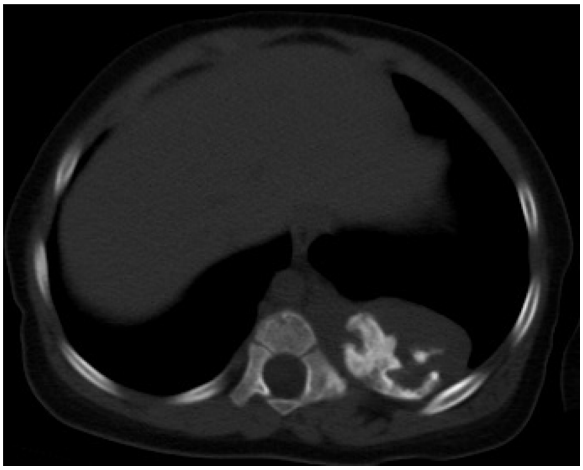

Fig. 1. Mesenchymal hamartoma in an 11-month-old. Axial chest CT image in bone windows shows a lobular, well-delineated, juxtapleural mass of the posterior left hemithorax with bizarre remodeling and enlargement of the involved rib.

2.2. Periosteal chondroma

Periosteal chondroma is a benign, slow-growing tumor of hyaline cartilage developing between the cortical surface of the bone and the periosteal membrane [23]. Periosteal chondromas rarely involve a rib and may be seen both in children and adults [24,25]. Periosteal chondromas account for less than 2% of all chondromas [25]. On clinical presentation a palpable mass with swelling and pain is typically seen, but painless masses have also been described [24]. Histopathologic examination demonstrates hyaline cartilage arranged in a lobular pattern closely associated with periosteum adjacent cortical bone [24]. Radiologic correlation in these cases is imperative to avoid misdiagnosis. Radiographically, periosteal chondroma usually arises on the outer surface of a long bone and manifests as a well-delineated, lobulated, radiolucent bone surface tumor, often with calcification of the chondroid matrix and a sclerotic reaction of the cortex (Fig. 2), classically, there is a saucer-shaped erosion of the cortex with adjacent bony sclerosis [25]. Ultrasound (US), CT and MRI are helpful to demonstrate the cartilaginous tissue and its relation with the surrounding structures. On MRI, the mass is bordered by a hypointense rim, corresponding to fibrous tissue and intact periosteum [25,26]. Differential diagnosis include osteochondroma, chondrosarcoma and osteosarcoma [24]. The treatment for periosteal chondroma is surgical excision [24,25].

2.3. Primitive myxoid mesenchymal tumor of infancy

Primitive myxoid mesenchymal tumor of infancy is a rare mesenchymal tumor of early childhood that can arise within the head/neck, trunk or extremities [27]. The incidence is unknown, but since it was first described in 2006, less than 20 reports of cases have been published in the literature [27,28]. The tumor is characterized **on histopathology** by predominantly round to bland or oval, less frequent stellate cells, and rare spindled cells in an abundant myxoid stroma with a fine "chicken-wire" vasculature [27–29]. Imaging findings include a heterogeneous infiltrative soft tissue mass with cystic-appearing spaces and no internal hemorrhage (Fig. 3) [27,29]. Differential diagnosis include sarcomas, myxoma, myxofibromas, and fibromatoses. The tumor has ill-defined borders with infiltration of surrounding structures. **The tumor** rarely metastases and has a poor response to chemotherapy; therefore, complete surgical resection is the recommended therapy, and close follow-up with serial MRI is **advised** to detect early recurrence [27].

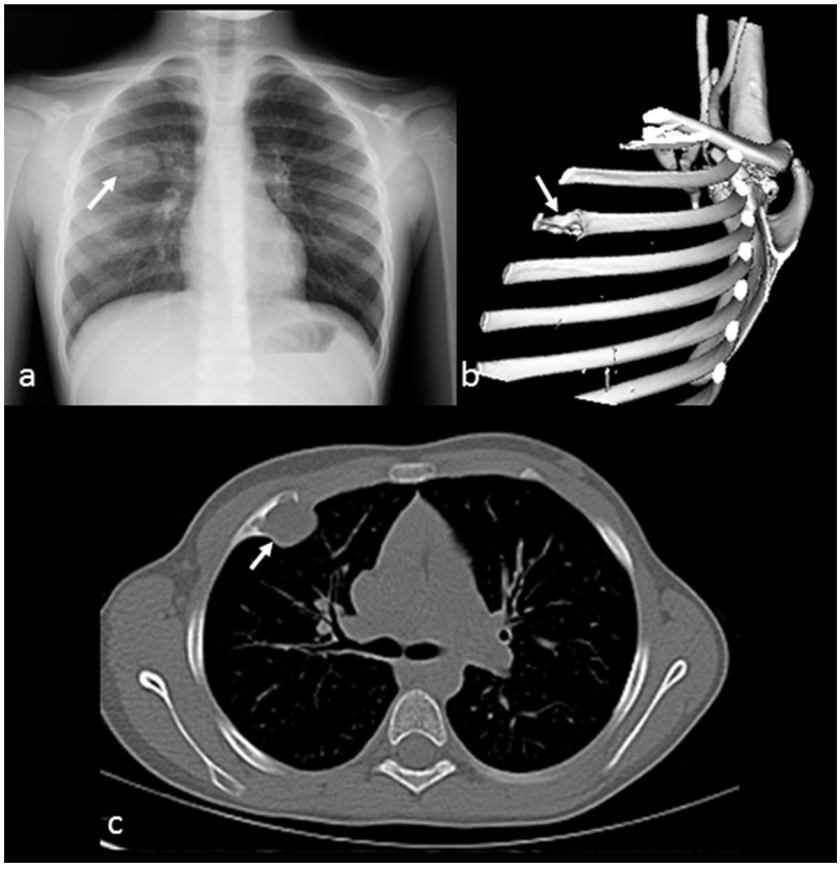

Fig. 2. Periosteal chondroma incidentally noted in a 6-year-old girl undergoing cardiac evaluation. (a) Frontal chest radiograph shows an opacity (arrow) projecting over the right lung. (b) Sagittal volume-rendered and (c) axial chest CT image in bone windows show a soft tissue mass (arrow) protruding from the third rib near the costochondral junction with **saucerization** and sclerosis of the adjacent bone.

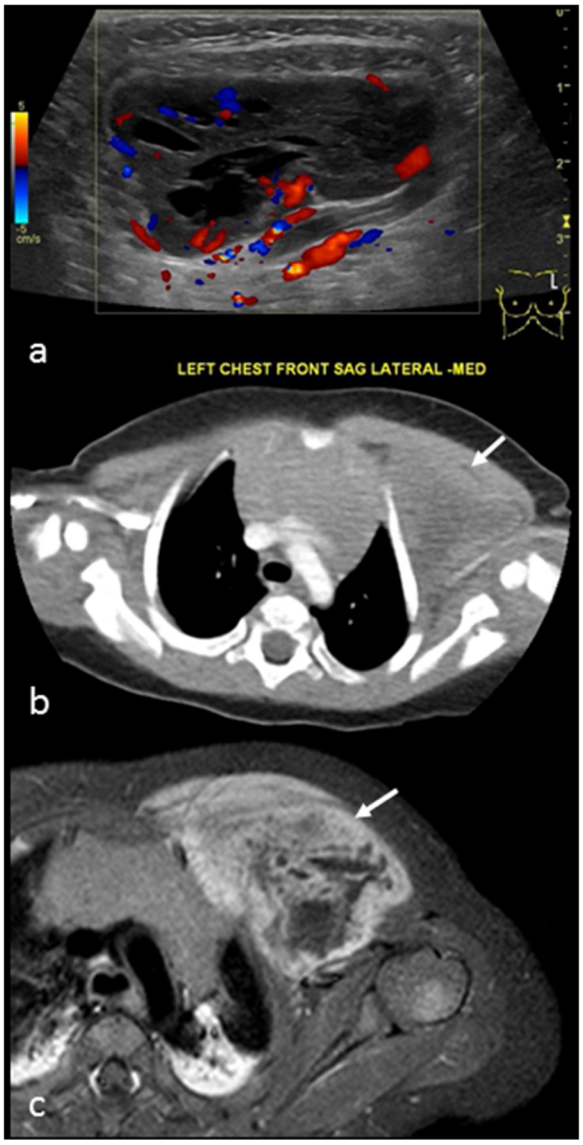

Fig. 3. Primitive myxoid mesenchymal tumor of infancy in a 3-month-old girl. (a) Doppler ultrasound shows a left upper chest wall mass with vascularized solid and fluid components. (b) Contrast-enhanced axial chest CT image demonstrates a mass (arrow) of heterogenous attenuation in the left anterior chest wall abutting the left second rib and pectoralis muscle. (c) Contrast-enhanced axial T1-weighted fat sat MRI image shows a mass (arrow) in the left anterior chest wall with enhancing solid tissue and non-enhancing myxoid stroma.

2.4. Chloroma

Chloroma, also known as granulocytic (myeloid) sarcoma or extramedullary myeloid leukemia, represents a mass of leukemic cells outside the bone marrow, and is most frequently associated with acute myelogenous leukemia (AML), chronic myeloid leukemia and other myeloproliferative disorders [30]. It is a rare condition with slight male predominance and may occur at any age, more commonly in infants than in older children and at any site of the body [10,31]. However, the skin, orbits, central nervous system, and paraspinous regions are the most common sites, with occasional presentations in the chest wall adjacent to the ribs and sternum [32]. Clinical presentation is dependent on tumor location, with symptoms usually occurring as a result of a tumor mass effect or local organ dysfunction [31]. Chloromas have a strong predilection for subperiosteal and perineural involvement (Fig. 4) [32]. **Histopathologic inspection shows that** the tumor is composed of primitive precursors of the granulocytic series that include myeloblasts, promyelocytes and myelocytes [30]. Typical imaging findings are **a high attenuation mass** with intense contrast enhancement on CT, iso-/hypointensity **on T1-weighted MRI**, mild hyperintensity on T2-weighted MRI, and restricted diffusion on diffusion weighted imaging (DWI) due to the high cellularity [32]. Fluorodeoxyglucose-positron emission tomography (FDG-PET) is useful because of its ability to detect the lesions that are clinically occult or not detectable on conventional imaging. Increased glycolytic activity with moderate FDG uptake is typical for these cases [33]. Differential diagnosis for the imaging findings is broad and includes lymphoma and sarcomas [32]. Systemic chemotherapy should be started early, even in the non-leukemic disease stage. Surgery and/or radiotherapy may be indicated for symptomatic lesions or tumors causing local organ dysfunction or obstruction [31]. Untreated isolated chloroma ultimately transforms to AML, typically over a 10- to 12-month period [31].

3. Lung parenchyma and airways

3.1. Infantile myofibromatosis

Infantile myofibromatosis is the most common fibrous tumor of infancy and is characterized by a benign proliferation of fibroblasts and myofibroblasts [34]. The tumor is subdivided into solitary and multicentric forms with or without visceral involvement [4,14]. Pulmonary involvement is rare, typically a manifestation of multicentric disease, and should not be misinterpreted as metastatic disease. The chest wall **can also be involved** [14,34]. The age of presentation is usually around 5 months for multicentric forms and 26 months for solitary forms [4]. On microscopic examination, these tumors have a nodular to multinodular proliferation with zonation, the peripheral zone of the nodule is composed of fascicles of "mature" spindled myofibroblasts without atypia or pleomorphisms, but occasional with mitotic figures. These tumor cells are embedded in a background of hyalinized to chondroid or chondromyxoid stroma. The central zone of the nodule is composed of "immature" ovoid to round spindled myofibroblasts associated with thin-walled branching vessels, imparting a hemangiopericytoma pattern [14]. On imaging, US demonstrates a thick-walled mass with an anechoic center that can resemble an abscess. On CT, the mass is nearly iso-attenuating to muscle, and on MRI the mass shows variable signal intensity on T2-weighted images with peripheral contrast enhancement (Fig. 5) [35,36]. The differential diagnosis is assisted by recognition of characteristic skeletal lesions in the multicentric form. Prognosis is worse in the multicentric forms with visceral involvement [14].

3.2. Fetal lung interstitial tumor

Fetal lung interstitial tumor is typically diagnosed in the prenatal or early postnatal period [37]. The tumor is composed of immature appearing microcystic lung tissue lined by cuboidal to low columnar epithelial cells (pneumocytes) with abundant cytoplasmic glycogen and lacking surfactant organelles. The supporting interstitial cells also contain abundant glycogen and are positive for vimentin. There are also smooth muscle cells beneath the epithelium with features resembling terminal bronchiole-alveolar ducts resemble immature fetal lung at 20–24 weeks of gestation [38,39]. Prenatal US shows a well-circumscribed, unifocal, predominantly solid lung mass with posterior acoustic enhancement (Fig. 6) [37,38,40,41]. Fetal MRI shows a well-circumscribed, intrathoracic mass that is hyperintense **on T2-weighted images** with radiating curved bands within and along the periphery of the lesion (Fig. 5) [37,38,41]. Fetal hydrops and heart failure are potential complications due to vena cava obstruction [41]. Findings on postnatal CXR are non-specific and include a lobar opacity with mediastinal shift [2]. Postnatal CT reveals a **low attenuation** mass without chest wall invasion [39]. Differential diagnosis include **solid (type 3)** congenital **pulmonary airway** malformation, congenital peribronchial

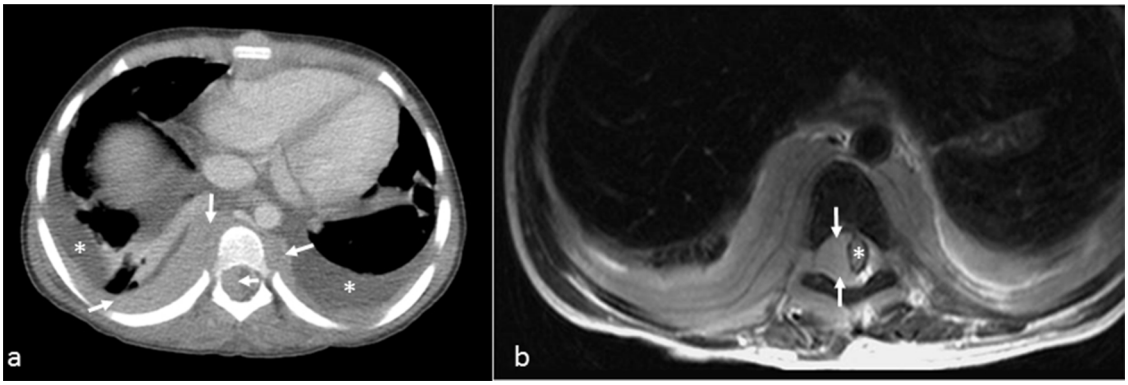

Fig. 4. Chloroma in a 4-year-old boy with history of relapsed acute myeloid leukemia. (a) Contrast-enhanced axial chest CT image shows bilateral pleural effusions (*) with a rind of **high attenuation** soft tissue (arrows) peripheral to the effusions adjacent to the posterior ribs and thoracic spine as well as adjacent to the sternum. (b) Contrast-enhanced axial T1-weighted MRI image more clearly shows extension of the soft tissue mass (arrows) into the thoracic spinal canal with displacement of the spinal cord (*).

Fig. 5. Infantile myofibromatosis in a 1-month-old girl. (a) Frontal body radiograph shows a well-circumscribed left lung mass (arrow) and characteristic symmetric lucent lesions (black arrows) of the metaphyses of the lower extremity long bones. (b) Contrast-enhanced axial chest CT image shows a well-circumscribed left pulmonary mass (arrow) with an attenuation similar to skeletal muscle. (c) Axial short T1 inversion recovery(STIR) MRI image shows a well-circumscribed left pulmonary mass (arrow) that is predominantly hyperintense with a hypointense rim.

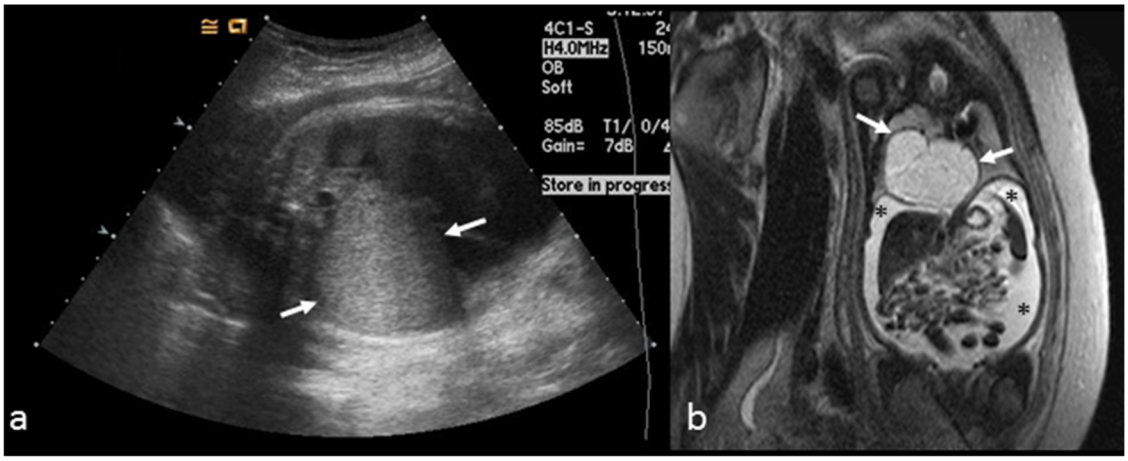

Fig. 6. Fetal lung interstitial tumor at 36 weeks gestation. (a) Prenatal ultrasound image depicts a large hyperechoic solid-appearing mass (arrows) of the right lung. (b) Coronal T2-weighted fetal MRI image shows compression of the lungs by a **well-circumscribed** hyperintense mass (arrows). In addition, fetal ascites (*) is noted.

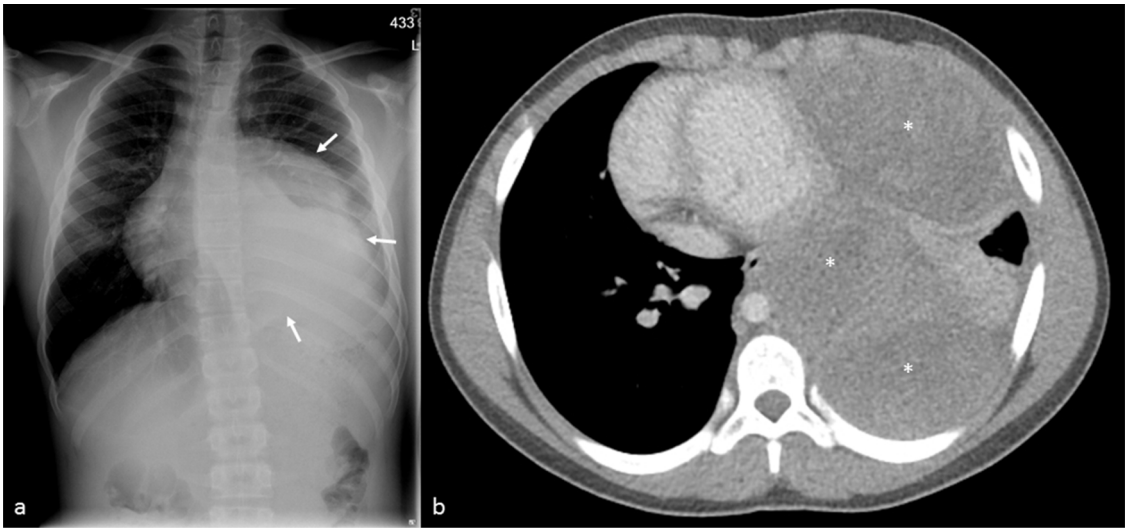

Fig. 7. Pleuropulmonary synovial sarcoma in a 13-year-old boy. (a) Frontal chest radiograph shows a large lobular mass (arrows) within the left mid and lower hemithorax obscuring the silhouette of the left heart border and hemidiaphragm. (b) Contrast-enhanced axial chest CT image demonstrates a large lobular mass (*) of heterogeneous attenuation abutting the cardiomediastinal structures and extending across the left hemithorax from the anterior to posterior pleura.

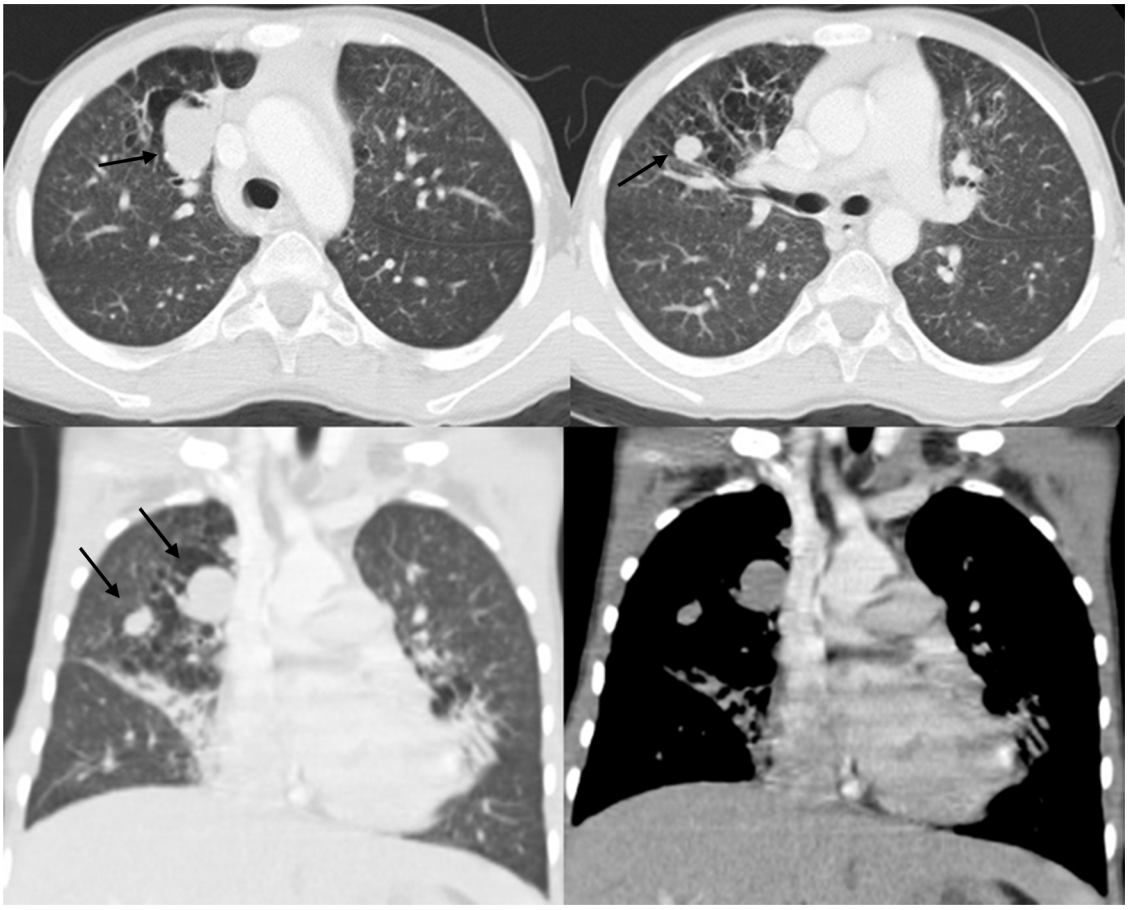

Fig. 8. Leiomyomas in an 11-year-old boy with history of acquired immunodeficiency syndrome (AIDS). Contrast-enhanced axial (a,b) chest CT images in lung windows and coronal (c,d) chest CT images in lung and soft tissue windows demonstrate multiple well-defined nodular pulmonary masses (black arrows) representing leiomyomas, as well as hyperlucent foci related to cystic lymphocytic interstitial pneumonia.

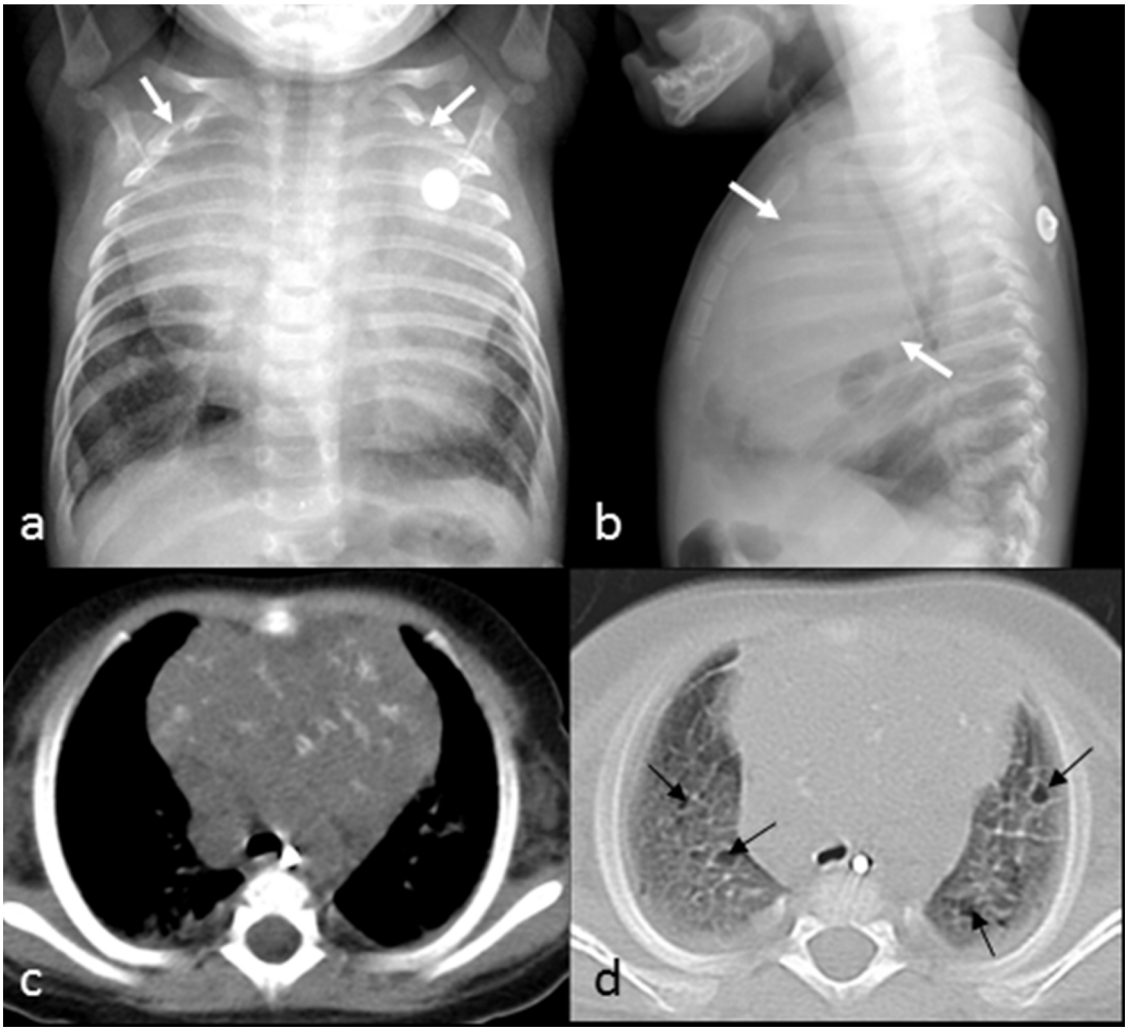

Fig. 9. Langerhans cell histiocytosis in a 3-month-old boy with history of cough and poor feeding. (a) Frontal and (b) lateral chest radiographs show a large mass (arrows) within the anterior mediastinum obscuring the silhouette of the upper heart border. (c) Non-contrast axial chest CT image shows a large anterior mediastinal mass with multiple **amorphous** calcifications. (d) Axial chest CT image in lung windows shows **multiple cystic lung lesions** (arrows).

myofibroblastic tumor and infantile pulmonary teratoid tumor [39]. Prognosis is favorable. Usually respiratory symptoms resolve without local recurrence or metastatic disease after surgical resection [38].

3.3. Pleuropulmonary synovial sarcoma

Pleuropulmonary synovial sarcoma is a subtype of sarcoma with a distinctive chromosomal translocation involving the X chromosome and chromosome 18 (SS18-SSX1; SS18-SSX2; SS18-SSX4) specific to synovial sarcoma [42–44]. It predominantly affects adolescents and young adults and represents 0.1 − 0.5% of all primary pulmonary malignancies [43]. Histologically, synovial sarcoma occurs in two different patterns: monophasic and biphasic. Monophasic synovial sarcoma is composed of malignant plump fusiform cells that are closely attached to one another, in a vague fascicular pattern with minimal stroma. Biphasic synovial sarcoma is composed of similar fusiform cells with area of gland-like epithelial structures lined by round to ovoid tumor cells [43,44]. On imaging, CXR typically shows a well-defined round or oval soft tissue mass of the lung or pleura, and is often accompanied by an ipsilateral pleural effusion [43]. CT reveals a well-circumscribed heterogeneously enhancing soft tissue mass without bone involvement or calcifications (Fig. 7) [45]. MRI provides superior demonstration of the enhancing nodular soft tissue component and multilocular fluid-filled component of the mass [43,46]. Differential diagnosis includes type II (mixed solid-cystic) pleuropulmonary blastoma, superinfected congenital lung malformation, and other sarcomas [4]. Current treatment consists of surgical resection followed by chemotherapy, radiotherapy, or both [43].

3.4. Leiomyoma and leiomyosarcoma

Leiomyoma and leiomyosarcoma of the pediatric lower respiratory tract are tumors of smooth muscle origin that exist along a benign to malignant spectrum and are associated with Epstein-Barr virus (EBV) infection and immunosuppressed states [47]. Patients usually present with nonspecific respiratory signs and symptoms [4]. Histologically, smooth muscle tumors are characterized by spindle cells with prominent eosinophilic cytoplasm, blunt end nuclei, and deep wrinkling of the nuclear membranes secondary to contraction artifact of the myofilaments during fixation. There is minimal cytologic atypia and rare to absent mitotic figures. The tumor cells occur in bundles or vague fascicles, and are closely apposed with minimal stroma. Transformation to malignant leiomyosarcoma is characterized by increased cellularity, marked pleomorphism, increased mitotic activity and invasion into adjacent tissues [14]. On imaging studies (Fig. 8) these tumors most commonly present as well-defined solid pulmonary or endobronchial masses [4]. These smooth muscle tumors are typically indolent and treated with surgery, chemotherapy or reduction in immunosuppression [47].

4. Mediastinum

4.1. Thymic Langerhans cell histiocytosis

Langerhans cell histiocytosis (LCH) is a rare disorder of unclear etiology characterized by proliferation and tissue infiltration by Langerhans cells with accompanying local and systemic inflammation [48,49]. The incidence of LCH is 2.6–5.4 cases per million children [50]. LCH presents a diagnostic challenge because it may manifest with a heterogeneous spectrum of lesions, ranging from a single bone lesion to multisystem disease. The thymus is commonly involved in pediatric LCH, especially in multisystem disease [51,52]. However, isolated thymic disease has rarely been reported in the literature [53]. Histologically, Langerhans cells are highly differentiated histiocytes of the stellate dendritic antigen-presenting cell lineage. The hallmark of LCH is an uncontrolled monoclonal proliferation of abnormal Langerhans cells, which may infiltrate nearly any tissue or organ as well as lymph nodes. This histiocytic infiltration is accompanied by chronic inflammation and the formation of granulomas [50]. On imaging, thymic involvement manifests as an enlarged thymus with or without cysts and amorphous calcifications on CXR or CT (Fig. 9) [51,52,54] and with heterogeneous uptake on FDG-PET [53]. US is an alternative method of assessing thymic involvement in patients younger than 2 years [51]. Differential diagnostic considerations of thymic LCH include lymphoma, **germ cell tumor,** juvenile xanthogranuloma and other forms of non-Langerhans cell histiocytosis [4,50]. Chemotherapy is the current standard of care for multisystem LCH, although progression-free survival among high-risk patients remains less than 50 % [49]. Children with liver, spleen, or bone marrow involvement are at highest risk for death from LCH [49].

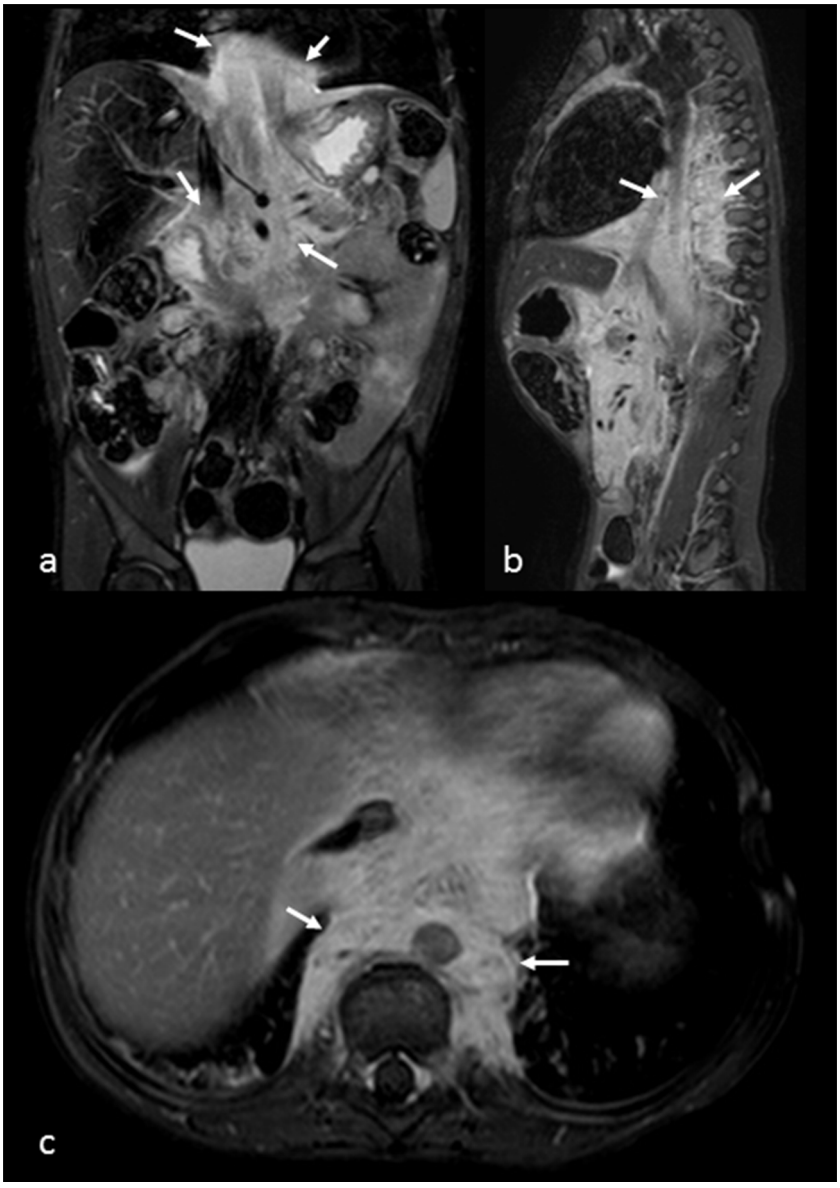

Fig. 10. Kaposiform hemangioendothelioma in a 4-year-old boy with Kasabach-Merritt syndrome. Contrast-enhanced (a) coronal, (b) sagittal, and (c) axial T1-weighted fat saturated MRI images demonstrate a poorly-defined enhancing soft tissue mass (arrows) infiltrating the lower mediastinum and upper retroperitoneum.

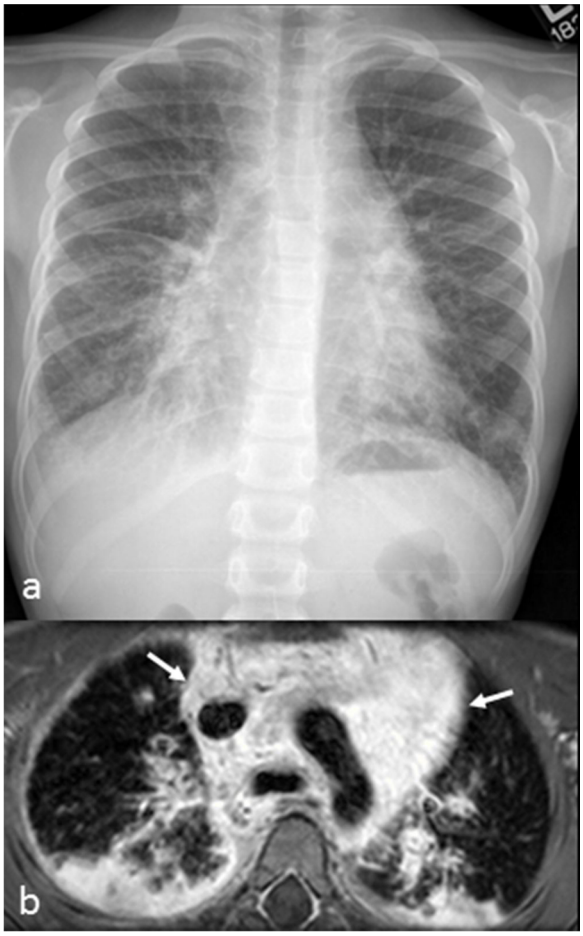

Fig. 11. Kaposiform lymphangiomatosis in a 6-year-old boy. (a) Frontal chest radiograph shows mediastinal widening and parahilar interstitial thickening. (b) Contrast-enhanced axial T1-weighted fat sat MRI image reveals extensive infiltration (arrows) of the mediastinum by enhancing soft tissue.

4.2. Kaposiform hemangioendothelioma

Kaposiform hemangioendothelioma is a locally aggressive vascular proliferation associated with Kasabach-Merritt phenomenon [55]. It occurs predominantly in infants and young children, most commonly as a superficial or deep soft tissue mass of the extremities or trunk, but may also occur in the head/neck, mediastinum, or retroperitoneum [55–59]. The risk of Kasabach-Merritt phenomenon increases dramatically when there is involvement of the mediastinum, retroperitoneum or muscle [58]. On histopathologic examination, the tumor is biphasic and composed of vascular and lymphatic components with irregular nodules of convoluted vessels and associated dense hyalinized stroma. The vessels are often associated with epithelioid and glomeruloid endothelial cell islands, resembling capillary hemangioma and Kaposi sarcoma. Hemosiderin deposition and fibrin thrombi are typically present [55]. On CT or MRI, Kaposiform hemangioendothelioma typically appears as an enhancing, infiltrative soft tissue mass with adjacent edema (Fig. 10) [59,60]. Differential diagnosis includes hemangioma and sarcomas. Intravenous corticosteroids, beta blockers, vincristine have proven to be effective [55].

4.3. Kaposiform lymphangiomatosis

Kaposiform lymphangiomatosis is an aggressive lymphatic disorder [61]. The mediastinum is involved in all thoracic cases, with the lungs and pleura also frequently involved. The age at presentation ranges from 3 months to 27 years [61]. The most common presenting symptom is respiratory compromise [61]. Histologically, it is characterized by clusters or sheets of spindled lymphatic endothelial cells accompanying malformed lymphatic channels that immunoreact with D240 [62]. The imaging features of Kaposiform lymphangiomatosis overlap with central conducting lymphatic anomaly and generalized lymphatic anomaly. On CT and MRI there is typically a mediastinal or retroperitoneal enhancing, infiltrative soft tissue lesion along the lymphatic distribution (Fig. 11) [61]. The mortality rate is high despite aggressive multi-modal therapy [62].

4.4. NUT carcinoma

NUT carcinoma (formerly NUT midline carcinoma) is a highly aggressive, poorly differentiated **subtype of squamous** carcinoma characterized by a translocation resulting in NUT oncogene overexpression [2,4,39,63]. It affects male and female patients equally, with a wide age distribution [63,64]. NUT carcinoma most commonly arises from the midline head/neck or mediastinum [64].The presenting symptoms are nonspecific and vary depending on the primary site of tumor or the presence of metastases [39]. Pleuritic chest pain, weight loss, nonproductive cough and shortness of breath are common when NUT carcinoma arises from thorax [65]. This entity is defined by rearrangement of the NUT gene (chromosome 15q14) with BRD4 (chromosome 19p31), most often, and on occasion with BRD3 (chromosome 9q34.2) [64]. Undifferentiated epithelioid to round cells with variable squamous differentiation are characteristic for this neoplasm, and there may be a degree of desmoplasia [63,64]. CT imaging demonstrates a heterogeneous mass with central necrosis and occasional calcifications (Fig. 12) [65–67]. On MRI, the tumor is hypointense on T1-weighted images, slightly hyperintense on T2-weighted images, and heterogeneously enhancing on post-contrast T1-weighted images [67]. FDG-PET is the imaging modality of choice for assessing for metastatic disease [66]. The lungs are the most common site of metastases and metastases to the liver, kidney, brain, spinal cord and subcutaneous soft tissues have been reported [4]. Differential diagnosis includes **tuberculosis**, histoplasmosis, neuroblastoma, lymphoma, sarcoma and IgG4-related disease. NUT carcinoma is almost always lethal [64].

5. Conclusion

Awareness of the spectrum of thoracic mass lesions is essential to provide optimal care for pediatric patients. **In addition to common entities, there are less common** malignant and benign neoplastic, non-neoplastic proliferative and hamartomatous lesions that may arise from the chest wall, lungs, or mediastinum. Differential diagnosis is aided by recognition of **their typical age distribution, presenting signs and symptoms, site of anatomic origin, and** imaging features.

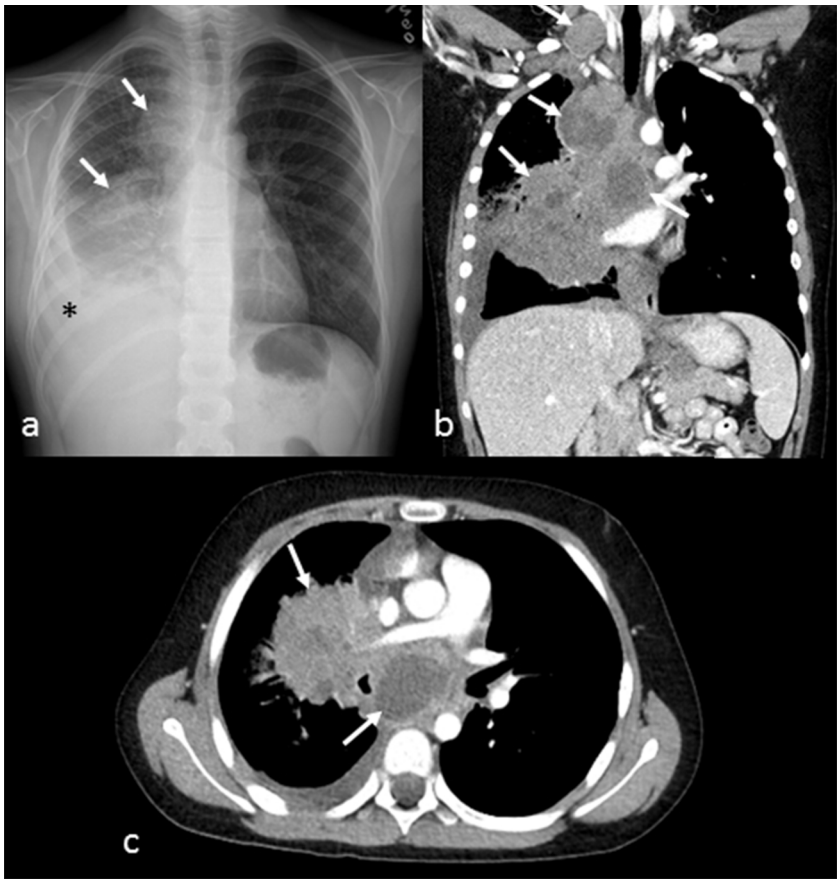

Fig. 12. Nuclear protein of the testis (NUT) carcinoma in a 12-year-old boy with a history of non-productive cough and weight loss. (a) Frontal chest radiograph demonstrates leftward displacement of the trachea by a right paratracheal mass (arrows), narrowing of the left mainstem bronchus, a right infrahilar mass (arrows) and a right pleural effusion (*). Contrast-enhanced (b) coronal and (c) axial CT images reveal centrally necrotic masses (arrows) in the paratracheal, subcarinal, right hilar and peribronchial nodal regions.

Declaration of Competing Interest

This manuscript is the original work of all authors, no part of this article has been published or presented before, nor is any part of it under consideration for publication elsewhere. This research did not receive any specific grant from funding agencies in the public, commercial, or not-for-profit sectors. There are no conflicts of interest to disclose. All authors have read and approved the final version of the manuscript.

Acknowledgment

None.

References

[1] M.C. Cohen, R.O. Kaschula, Primary pulmonary tumors in childhood: a review of 31 years' experience and the literature, Pediatr. Pulmonol. 14 (1992) 222–232.
[2] J.Pr. Lichtenberger, D.M. Biko, B.W. Carter, M.A. Pavio, A.R. Huppmann, E.M. Chung, Primary lung tumors in children: radiologic-pathologic correlation from the radiologic pathology archives, Radiographics 38 (2018) 2151–2172.
[3] B.J. Hancock, M. Di Lorenzo, S. Youssef, S. Yazbeck, J.E. Marcotte, P.P. Collin, Childhood primary pulmonary neoplasms, J. Pediatr. Surg. 28 (1993) 1133–1136.
[4] K. Lyons, R.P. Guillerman, K. McHugh, Pulmonary and extrathymic mediastinal tumors, in: P. Garcia-Peña, R.P. Guillerman (Eds.), Pediatric Chest Imaging, Springer, Verlag Berlin Heidelberg, 2014, pp. 349–371.
[5] M. Paulussen, S. Ahrens, A.W. Craft, J. Dunst, B. Frohlich, S. Jabar, C. Rube, W. Winkelmann, S. Wissing, A. Zoubek, H. Jurgens, Ewing's tumors with primary lung metastases: survival analysis of 114 (European Intergroup) Cooperative Ewing's Sarcoma Studies patients, J. Clin. Oncol. 16 (1998) 3044–3052.
[6] S.C. Kaste, C.B. Pratt, A.M. Cain, D.J. Jones-Wallace, B.N. Rao, Metastases detected at the time of diagnosis of primary pediatric extremity osteosarcoma at diagnosis: imaging features, Cancer 86 (1999) 1602–1608.
[7] F. Cowie, R. Corbett, C.R. Pinkerton, Lung involvement in neuroblastoma: incidence and characteristics, Med. Pediatr. Oncol. 28 (1997) 429–432.
[8] S.G. Dubois, W.B. London, Y. Zhang, K.K. Matthay, T. Monclair, P.F. Ambros, S.L. Cohn, A. Pearson, L. Diller, Lung metastases in neuroblastoma at initial diagnosis: a report from the International Neuroblastoma Risk Group (INRG) project, Pediatr. Blood Cancer 51 (2008) 589–592.
[9] J. Fuchs, G. Seitz, R. Handgretinger, J. Schafer, S.W. Warmann, Surgical treatment of lung metastases in patients with embryonal pediatric solid tumors: an update, Semin. Pediatr. Surg. 21 (2012) 79–87.
[10] R.P. Guillerman, S.D. Voss, B.R. Parker, Leukemia and lymphoma, Radiol. Clin. North Am. 49 (2011) 767–797.
[11] G.L. Hedlund, J.F. Navoy, C.A. Galliani, W.H. Johnson Jr., Aggressive manifestations of inflammatory pulmonary pseudotumor in children, Pediatr. Radiol. 29 (1999) 112–116.
[12] F. Mergan, F. Jaubert, F. Sauvat, O. Hartmann, S. Lortat-Jacob, Y. Revillon, C. Nihoul-Fekete, S. Sarnacki, Inflammatory myofibroblastic tumor in children: clinical review with anaplastic lymphoma kinase, Epstein-Barr virus, and human herpesvirus 8 detection analysis, J. Pediatr. Surg. 40 (2005) 1581–1586.
[13] D.N. Miniati, M. Chintagumpala, C. Langston, M.K. Dishop, O.O. Olutoye, J.G. Nuchtern, D.L. Cass, Prenatal presentation and outcome of children with pleuropulmonary blastoma, J. Pediatr. Surg. 41 (2006) 66–71.
[14] M.K. Dishop, S. Kuruvilla, Primary and metastatic lung tumors in the pediatric population: a review and 25-year experience at a large children's hospital, Arch. Pathol. Lab. Med. 132 (2008) 1079–1103.
[15] A.E. Hosman, E.M. de Gussem, W.A.F. Balemans, A. Gauthier, C.J.J. Westermann, R.J. Snijder, M.C. Post, J.J. Mager, Screening children for pulmonary arteriovenous malformations: evaluation of 18 years of experience, Pediatr. Pulmonol. 52 (2017) 1206–1211.
[16] P. Garcia-Pena, A. Coma, G. Enriquez, Congenital lung malformations: radiological findings and clues for differential diagnosis, Acta Radiol. 54 (2013) 1086–1095.
[17] A.R. Al-Qahtani, M. Di Lorenzo, S. Yazbeck, Endobronchial tumors in children: institutional experience and literature review, J. Pediatr. Surg. 38 (2003) 733–736.
[18] E.M. Dulmet, P. Macchiarini, B. Suc, J.M. Verley, Germ cell tumors of the mediastinum. A 30-year experience, Cancer 72 (1993) 1894–1901.
[19] A.G. Ayala, J.Y. Ro, A. Bolio-Solis, F. Hernandez-Batres, F. Eftekhari, J. Edeiken, Mesenchymal hamartoma of the chest wall in infants and children: a clinicopathological study of five patients, Skeletal Radiol. 22 (1993) 569–576.
[20] T. Tanaka, S. Fumino, T. Shirai, E. Konishi, T. Tajiri, Mesenchymal hamartoma of the chest wall in a 10-year-old girl mimicking malignancy: a case report, Skeletal Radiol. 48 (2019) 643–647.
[21] G.F. Eich, C.J. Kellenberger, U.V. Willi, Radiology of the chest Wall, in: P. Garcia-Peña, R.P. Guillerman (Eds.), Pediatric Chest Imaging, Springer, Verlag Berlin Heidelberg, 2014, pp. 431–458.
[22] K.R. Groom, M.D. Murphey, L.M. Howard, G.J. Lonergan, M.L. Rosado-De-Christenson, A.H. Torop, Mesenchymal hamartoma of the chest wall: radiologic manifestations with emphasis on cross-sectional imaging and histopathologic

comparison, Radiology 222 (2002) 205–211.
[23] E.W. Brien, J.M. Mirra, J.V. Luck Jr., Benign and malignant cartilage tumors of bone and joint: their anatomic and theoretical basis with an emphasis on radiology, pathology and clinical biology. II. Juxtacortical cartilage tumors, Skeletal Radiol. 28 (1999) 1–20.
[24] S. Inoue, S. Fujino, K. Kontani, S. Sawai, N. Tezuka, J. Hanaoka, Periosteal chondroma of the rib: report of two cases, Surg. Today 31 (2001) 1074–1078.
[25] R. Karabakhtsian, D. Heller, M. Hameed, C. Bethel, Periosteal chondroma of the rib–report of a case and literature review, J. Pediatr. Surg. 40 (2005) 1505–1507.
[26] F. Lorente, D.J. Molto, V. Bonete Lluch, Marti Perales, Childhood periosteal chondroma, Arch Orthop Trauma Surg 120 (2000) 605–608.
[27] J.H. Foster, S.A. Vasudevan, M. John Hicks, D. Schady, M. Chintagumpala, Primitive myxoid mesenchymal tumor of infancy involving chest wall in an infant: a case report and clinicopathologic correlation, Pediatr. Dev. Pathol. 19 (2016) 244–248.
[28] R. Alaggio, V. Ninfo, A. Rosolen, C.M. Coffin, Primitive myxoid mesenchymal tumor of infancy: a clinicopathologic report of 6 cases, Am. J. Surg. Pathol. 30 (2006) 388–394.
[29] A.A. Saeed, Q. Riaz, N.U. Din, S. Altaf, Primitive myxoid mesenchymal tumor of infancy with brain metastasis: first reported case, Childs Nerv. Syst. 35 (2019) 363–368.
[30] C.S. Wilson, L.J. Medeiros, Extramedullary manifestations of myeloid neoplasms, Am. J. Clin. Pathol. 144 (2015) 219–239.
[31] L.M. Almond, M. Charalampakis, S.J. Ford, D. Gourevitch, A. Desai, Myeloid sarcoma: presentation, diagnosis, and treatment, Clin. Lymphoma Myeloma Leuk. 17 (2017) 263–267.
[32] G.S. Shroff, M.T. Truong, B.W. Carter, M.F. Benveniste, R. Kanagal-Shamanna, G. Rauch, C. Viswanathan, P.C. Boddu, N. Daver, C.C. Wu, Leukemic involvement in the thorax, Radiographics 39 (2019) 44–61.
[33] E.Y. Lee, M.P. Anthony, A.Y. Leung, F. Loong, P.L. Khong, Utility of FDG PET/CT in the assessment of myeloid sarcoma, AJR Am. J. Roentgenol. 198 (2012) 1175–1179.
[34] M. Gopal, G. Chahal, Z. Al-Rifai, B. Eradi, G. Ninan, S. Nour, Infantile myofibromatosis, Pediatr. Surg. Int. 24 (2008) 287–291.
[35] K. Koujok, R.E. Ruiz, R.J. Hernandez, Myofibromatosis: imaging characteristics, Pediatr. Radiol. 35 (2005) 374–380.
[36] L. Naffaa, I. Khalifeh, R. Salman, M. Itani, R. Saab, A. Al-Kutoubi, Infantile myofibromatosis: review of imaging findings and emphasis on correlation between MRI and histopathological findings, Clin. Imaging 54 (2019) 40–47.
[37] J. Phillips, A. Blask, A.D. Brahmbhatt, A. Lawrence, J. Timofeev, A. Badillo, N. Andescavage, Fetal lung interstitial tumor: prenatal presentation of a rare fetal malignancy, J. Neonatal. Med. (2019).
[38] M.K. Dishop, E.M. McKay, P.A. Kreiger, J.R. Priest, G.M. Williams, C. Langston, J. Jarzembowski, M. Suchi, L.P. Dehner, D.A. Hill, Fetal lung interstitial tumor (FLIT): a proposed newly recognized lung tumor of infancy to be differentiated from cystic pleuropulmonary blastoma and other developmental pulmonary lesions, Am. J. Surg. Pathol. 34 (2010) 1762–1772.
[39] R.P. Guillerman, E. Vogelius, A. Pinto-Rojas, D.M. Parham, Malignancies of the pediatric Lower respiratory tract, in: D.M. Parham, J.D. Khoury, M.B. McCarville (Eds.), Pediatric Malignancies: Pathology and Imaging, Springer, Verlag New York, 2015, pp. 227–243.
[40] M. Yoshida, M. Tanaka, K. Gomi, T. Iwanaka, L.P. Dehner, Y. Tanaka, Fetal lung interstitial tumor: the first Japanese case report and a comparison with fetal lung tissue and congenital cystic adenomatoid malformation/congenital pulmonary airway malformation type 3, Pathol. Int. 63 (2013) 506–509.
[41] D.A. Lazar, D.L. Cass, M.K. Dishop, K. Adam, O.A. Olutoye, N.A. Ayres, C.I. Cassady, O.O. Olutoye, Fetal lung interstitial tumor: a cause of late gestation fetal hydrops, J. Pediatr. Surg. 46 (2011) 1263–1266.
[42] L. Yuan, Z. Guan, X. Dai, J. Xu, Primary pleuropulmonary synovial sarcoma: a case report, Int. J. Clin. Exp. Pathol. 8 (2015) 15426–15428.
[43] A.A. Frazier, T.J. Franks, R.D. Pugatch, J.R. Galvin, From the archives of the AFIP: pleuropulmonary synovial sarcoma, Radiographics 26 (2006) 923–940.
[44] T. Lan, H. Chen, B. Xiong, T. Zhou, R. Peng, M. Chen, F. Ye, J. Yao, X. He, Y. Wang, H. Zhang, Primary pleuropulmonary and mediastinal synovial sarcoma: a clinicopathologic and molecular study of 26 genetically confirmed cases in the largest institution of southwest China, Diagn. Pathol. 11 (2016) 62.
[45] W.D. Zhang, Y.B. Guan, Y.F. Chen, C.X. Li, CT imaging of primary pleuropulmonary synovial sarcoma, Clin. Radiol. 67 (2012) 884–888.
[46] M. Mirzoyan, A. Muslimani, S. Setrakian, M. Swedeh, H.A. Daw, Primary pleuropulmonary synovial sarcoma, Clin. Lung Cancer 9 (2008) 257–261.
[47] D.M. Parham, R. Alaggio, C.M. Coffin, Myogenic tumors in children and adolescents, Pediatr. Dev. Pathol. 15 (2012) 211–238.
[48] J.J. Junewick, N.E. Fitzgerald, The thymus in Langerhans' cell histiocytosis, Pediatr. Radiol. 29 (1999) 904–907.
[49] C.E. Allen, M. Merad, K.L. McClain, Langerhans-cell histiocytosis, N. Engl. J. Med. 379 (2018) 856–868.
[50] S. Schmidt, G. Eich, A. Geoffray, S. Hanquinet, P. Waibel, R. Wolf, I. Letovanec, L. Alamo-Maestre, F. Gudinchet, Extraosseous langerhans cell histiocytosis in children, Radiographics 28 (2008) 707–726.
[51] K. Lakatos, H. Herbruggen, U. Potschger, H. Prosch, M. Minkov, Radiological features of thymic langerhans cell histiocytosis, Pediatr. Blood Cancer 60 (2013) E143–145.
[52] S. Ducassou, F. Seyrig, C. Thomas, A. Lambilliotte, P. Marec-Berard, C. Berger, G. Plat, L. Brugiere, M. Ouache, M. Barkaoui, C. Armari-Alla, P. Lutz, G. Leverger, X. Rialland, L. Mansuy, H. Pacquement, E. Jeziorski, V. Gandemer, F. Chalard, J.F. Chateil, A. Tazi, J.F. Emile, J. Donadieu, Thymus and mediastinal node involvement in childhood Langerhans cell histiocytosis: long-term follow-up from the French national cohort, Pediatr. Blood Cancer 60 (2013) 1759–1765.
[53] S. Turpin, A.S. Carret, J. Dubois, C. Buteau, N. Patey, Isolated thymic Langerhans cell histiocytosis discovered on F-18 fluorodeoxyglucose positron emission tomography/computed tomography (F-18 FDG PET/CT), Pediatr. Radiol. 45 (2015) 1870–1873.
[54] G.D. Heller, J.O. Haller, W.E. Berdon, S. Sane, P.K. Kleinman, Punctate thymic calcification in infants with untreated Langerhans' cell histiocytosis: report of four new cases, Pediatr. Radiol. 29 (1999) 813–815.
[55] L.L. Lyons, P.E. North, F. Mac-Moune Lai, M.H. Stoler, A.L. Folpe, S.W. Weiss, Kaposiform hemangioendothelioma: a study of 33 cases emphasizing its pathologic, immunophenotypic, and biologic uniqueness from juvenile hemangioma, Am. J. Surg. Pathol. 28 (2004) 559–568.
[56] M.A. Veening, J.I. Verbeke, M.M. Witbreuk, G.J. Kaspers, Kaposiform (spindle cell) hemangioendotelioma in a child with an unusual presentation, J. Pediatr. Hematol. Oncol. 32 (2010) 240–242.
[57] T. Nakaya, K. Morita, A. Kurata, T. Ushiku, T. Igarashi, M. Kuroda, M. Fukayama, Multifocal kaposiform hemangioendothelioma in multiple visceral organs: an autopsy of 9-day-old female baby, Hum. Pathol. 45 (2014) 1773–1777.
[58] S.E. Croteau, M.G. Liang, H.P. Kozakewich, A.I. Alomari, S.J. Fishman, J.B. Mulliken, C.C. Trenor 3rd., Kaposiform hemangioendothelioma: atypical features and risks of Kasabach-Merritt phenomenon in 107 referrals, J. Pediatr. 162 (2013) 142–147.
[59] Y.J. Chen, C.K. Wang, Y.C. Tien, T.J. Hsieh, MRI of multifocal kaposiform haemangioendothelioma without Kasabach-Merritt phenomenon, Br. J. Radiol. 82 (2009) e51–54.
[60] Y.J. Ryu, Y.H. Choi, J.E. Cheon, W.S. Kim, I.O. Kim, J.E. Park, Y.J. Kim, Imaging findings of Kaposiform Hemangioendothelioma in children, Eur. J. Radiol. 86 (2017) 198–205.
[61] P. Goyal, A.I. Alomari, H.P. Kozakewich, C.C. Trenor 3rd., A.R. Perez-Atayde, S.J. Fishman, A.K. Greene, R. Shaikh, G. Chaudry, Imaging features of kaposiform lymphangiomatosis, Pediatr. Radiol. 46 (2016) 1282–1290.
[62] S.E. Croteau, H.P. Kozakewich, A.R. Perez-Atayde, S.J. Fishman, A.I. Alomari, G. Chaudry, J.B. Mulliken, C.C. Trenor 3rd., Kaposiform lymphangiomatosis: a distinct aggressive lymphatic anomaly, J. Pediatr. 164 (2014) 383–388.
[63] C.A. French, NUT midline carcinoma, Cancer Genet. Cytogenet. 203 (2010) 16–20.
[64] C.A. French, The importance of diagnosing NUT midline carcinoma, Head Neck Pathol. 7 (2013) 11–16.
[65] R.J. Bair, J.F. Chick, N.R. Chauhan, C. French, R. Madan, Demystifying NUT midline carcinoma: radiologic and pathologic correlations of an aggressive malignancy, AJR Am. J. Roentgenol. 203 (2014) W391–399.
[66] D.G. Rosenbaum, J. Teruya-Feldstein, A.P. Price, P. Meyers, S. Abramson, Radiologic features of NUT midline carcinoma in an adolescent, Pediatr. Radiol. 42 (2012) 249–252.
[67] A. Polsani, K.A. Braithwaite, A.L. Alazraki, C. Abramowsky, B.M. Shehata, NUT midline carcinoma: an imaging case series and review of literature, Pediatr. Radiol. 42 (2012) 205–210.